DOI: 10.1002/chem.200501321

# Aromaticity of Giant Polycyclic Aromatic Hydrocarbons with Hollow Sites: Super Ring Currents in Super-Rings

**Balázs Hajgató,[a] Michael S. Deleuze,[b] and Koichi Ohno*[a]**

**Abstract:** We present a systematic theoretical study based on semi-empirical, Hartree–Fock (HF), and density functional theory (DFT) models of a series of polycyclic aromatic hydrocarbons (PAHs) that exhibit hollow sites. In this study we focus particularly on the magnetic criteria of aromaticity, namely $^1$H NMR and nucleus-independent chemical shifts (NICS), and on their relationships with other electronic properties. The computed shifts and NICS indices indicate that an external magnetic field induces exceptionally strong ring currents in even-layered PAH doughnuts, in particular in the layer directly adjacent to the central hole of double-layered compounds. These exceptionally strong ring currents also correlate with particularly small HOMO–LUMO gaps and electronic excitation energies and to abnormally high polarizabilities, indicating in turn that these compounds have a more pronounced metallic character. Comparison is made with further depictions of aromaticity in these systems and in [18]–[66]annulene rings by employing topological, structural, and energetic criteria.

**Keywords:** ab initio calculations · aromaticity · polarizabilities · polycyclic aromatic hydrocarbons · ring currents

## Introduction

Polycyclic aromatic hydrocarbons (PAHs) consist of two or more condensed aromatic rings of carbon atoms, to which are attached peripheral hydrogen atoms. PAHs have long been the focus of both theoretical and experimental research owing to their importance in several fields of science. They occur in nature mostly in traces embedded in different materials and their origin can be natural or may be connected to human activities. Numerous different PAHs are present in petroleum samples and they are also produced in the burning of mineral oil derivatives.[1] Nowadays the main fuel for internal combustion engines is mineral oil derivatives, hence PAHs form an important group of extremely hazardous environmental pollutants and some of them are also highly cancerous.[2] PAHs have also been identified in various extraterrestrial environments. Nowadays they are commonly accepted as being ubiquitous in the interstellar medium[3] and are regarded as being responsible for some of the diffuse interstellar bands and unidentified emission bands in the mid-IR range.[4–6] Large PAHs are frequently used for modelling graphite sheets and glassy carbon materials.[7] Last but not least, a few PAHs are known to be very suitable for the making of conducting organic materials that can be used to produce cheap but efficient electronic devices such as organic thin-film transistors.[8]

A number of PAHs, mainly of small and moderate size, have been synthesized. Gigantic PAHs containing 114[9] and 222[10] carbon atoms have recently be produced.[11] The extremely limited solubility of large PAHs is clearly a serious obstacle to the synthesis and structural characterization of new and exotic PAHs. Indeed, the solubility of large PAHs drastically decreases with size and the recently synthesized large PAHs have been reported to be completely insoluble.[9,10] Experimental progress in this field is slow, but has been significant enough to motivate a wealth of theoretical studies on the electronic structure and spectra of PAHs as well as on their radical cations and anions. These studies range from semiempirical[12–15] to ab initio[16–20] methods and include DFT levels of theory.[15,19–22]

A key but highly controversial concept used in discussions on the structure and physicochemical properties of these

[a] Dr. B. Hajgató, Prof. Dr. K. Ohno
Department of Chemistry, Graduate School of Science
Tohoku University
6-3 Aramaki, Aza-aoba, Aoba-ku, Sendai 980-8578 (Japan)
Fax: (+81) 22-795-6580
E-mail: ohnok@qpcrkk.chem.tohoku.ac.jp

[b] Prof. Dr. M. S. Deleuze
Group of Theoretical Chemistry, Department SBG
Hasselt University
Universitaire Campus, B-3590 Diepenbeek (Belgium)

Supporting information for this article is available on the WWW under http://www.chemeurj.org/ or from the author.

  

compounds as well as their reactions is that of aromaticity. Almost every chemist agrees that PAHs are aromatic but that the degree of aromaticity may differ strongly from one system to another. The notion of aromaticity originates from the fact that benzene, the very prototype of all aromatic molecules, as well as many of its derivatives, are known to have strong fragrance.[23] Aromaticity is not a directly measurable quantity and it has as yet no commonly accepted quantitative definition but on the contrary is described according to many variant concepts or criteria (for example, spherical aromaticity,[24] homoaromaticity,[25] magnetic aromaticity and ring currents,[26,27] structural aromaticity,[28] chemical hardness[29] and reactivity,[30] Dewar resonance energy,[31] $\pi$ distortivity,[32] and chemical graph theories,[33,34]). Note that the extent of "aromaticity" in PAH compounds may strongly vary from one system to another, and describing them as polycyclic benzenoid hydrocarbons has therefore often been advocated.

Organic chemists most often define aromaticity from reactivity rules. According to these aromaticity denotes great stability and a much greater propensity to undergo electrophilic substitutions rather than additions to the aromatic core. Following the classification by Katritzky and co-workers,[35] the quantitative criteria of aromaticity are nowadays most commonly divided into three classes: energetic, magnetic, and geometric. According to the definition based on energetic criteria aromatic compounds are characterized by large and positive aromatic stabilization energies (ASE).[36] The magnetic interpretation of aromaticity relates to the fact that an external magnetic field induces diatropic $\pi$ ring currents resulting in a local shielding of the field.[37] The simple connection between ring currents and aromaticity was first suggested by Elvidge and Jackman in the early 1960s.[38,39] This relationship was extensively studied in the seventies and eighties.[40–44] Interested readers are referred to references [45–47] for general reviews on the ring-current effect. In their pioneering work, Wilcox and co-workers correlated aromaticity and ring currents to geometric parameters.[48–50] From a structural viewpoint, the main characteristic of aromatic systems is their tendency to exhibit bond-length equalization.[51] Some earlier work on rather limited sets of PAHs led to the conclusion that the latter three (physicochemical) definitions of aromaticity correlate well with each other.[52,53] Studies on larger sets of PAHs have more recently shown that the phenomenon of aromaticity should rather be regarded as being statistically multidimensional.[54] At last it is also possible to characterize aromaticity on purely topological grounds using, for instance, the mathematical discipline of chemical graph theory.[33,34,55–61] In addition to the previously mentioned and most commonly used methods there are other ways to describe aromaticity.[62,63]

In our previous paper[15] we described a new series of giant PAHs with hollow sites with some of these having special properties reflecting various degrees of aromaticity. The special properties to which we refer are in some cases exceptionally low singlet-ground-state lowest-singlet-excited-state ($S_0$–$S_1$) transition energies, which, rather than varying monotonically, exhibit strong and rather unexpected fluctuations with increasing system size. The main purpose of this work was to investigate in more detail the interplay between the molecular and electronic structures of these compounds by resorting to the most commonly accepted magnetic, structural, and energetic criteria of aromaticity. It is worth recalling at this stage that magnetic indices of aromaticity such as NMR chemical shifts or $\pi$ ring currents are molecular responses[64–66] to an external perturbation (in this case a homogeneous magnetic field) and that as such they are intimately related to the propensity of the molecule to undergo electronic excitations. Another example of a (linear) response to an external perturbation is that of the dipole electric polarizability tensor ($\vec{\vec{\alpha}}$), which is a measure of the first-order variation of the molecular dipole moment ($\vec{\mu}_0$) in a homogeneous external electric field ($\vec{\mu} = \vec{\mu}_0 + \vec{\vec{\alpha}}\vec{F} + \ldots$) and as such has been extensively used to design conjugated materials suited for applications in optoelectronics.[67] A second purpose of this work therefore was to show that, since they relate to low electronic HOMO–LUMO gaps, high magnetic indices of aromaticity also correlate with low electronic excitation energies, higher electric polarizabilities, as well as with a stronger propensity to undergo symmetry-lowering in theoretical calculations in order to release near-energy degeneracies, in particular at lower levels that do not cope with electron correlation. In simple words, we aimed to prove that for large hollow PAHs, high magnetic indices of aromaticity may also simply denote a rather pronounced metallic character because large molecular responses to an external perturbation, be it an electric or magnetic field, are basic characteristics of metallic materials.

## Computational Methods

All calculations were carried out using the Gaussian 03 program package.[68] All geometries were optimized first at the RHF/6-31G and/or RB3LYP/6-31G levels of theory, to start with under the constraint of $D_{6h}$ symmetry point groups. The stability of the identified stationary points was systematically checked by computing the harmonic vibrational spectrum at the same theoretical levels. At the B3LYP/6-31G level of theory, $D_{6h}$ structures characterized by imaginary vibrational frequencies were systematically reoptimized under the constraints of lower point groups until true energy minima were obtained. The symmetry of these minima was retained for further geometry optimizations and frequency calculations at the HF/6-31G level of theory, without this time modifying the symmetry to a lower point group if the latter calculations revealed a saddle-point. Infra-red intensities were computed at the same levels of theory from squared derivatives of the total energy over Cartesian coordinates and over an external homogeneous electric field, according to the double harmonic approximation.[64] In practice the latter implies calculations of the dipole electric polarizability tensor $\vec{\vec{\alpha}}$ using coupled perturbed Hartree–Fock (CPHF) theory[69] or its DFT-B3LYP version. At this stage, it is worth recalling that B3LYP geometries and vibrational frequencies are known to be of a quality comparable to that achieved with many-body ab initio treatments at the confines of nonrelativistic quantum mechanics, such as CCSD(T).[70,71]

$^1$H NMR chemical shifts and NICS indices[72–74] were calculated using the gauge-independent atomic orbital (GIAO) approach[75] in conjunction

  

with the B3LYP/6-31G level of theory. We also performed these calculations at the HF/6-31G level of theory using CNDO ($D_{6h}$) geometries to make comparison with the results of our previous paper[15] and thereby compare the quality of the HF and DFT calculations. NICS(0) values (calculated in the ring centers) do not depend purely on ring currents within the π system but also on other contributions to magnetic shielding due to local circulations of electrons in bonds, lone pairs, and even atom cores. The interference from these local currents is reduced above the ring centers so NICS(1) values (calculated 1 Å above the ring centers) were used because they more specifically describe π resonance effects.[72,73] Aromatic and antiaromatic systems are characterized by large negative and positive NICS(1) values, respectively, whereas NICS(1) values around zero are typically found for nonaromatic systems (−10.4 for benzene, +16.1 for cyclobutadiene, and +0.9 for *p*-benzoquinone at the B3LYP/6-31G level of theory). The $^1$H NMR chemical shifts were calculated relative to $CH_4$. In these calculations we assumed that the calculated gas-phase absolute isotropic magnetic shielding of hydrogen atoms in $CH_4$ is equal to the solvent-phase experimental $^1$H NMR chemical shift of $CH_4$.[76]

The lowest excitation energies were calculated from CNDO geometries using the CIS-ZINDO-S method. Compared with experiment and with more robust but in this case completely intractable theoretical treatments of electronic excitation processes such as TD-DFT and CASSCF, this rather simple CIS-ZINDO-S approach is known[77] to provide quantitatively fairly reliable results (0.2 eV accuracy) for low-lying singly excited states. Very clearly, when applied to extremely large PAHs, the accuracy of the CIS-ZINDO-S excitation energies strongly depends on the configuration interaction (CI) space employed.[15] In this work, 200 electrons were allowed to excite over a CI active space of 200 orbitals (or less if the target systems have fewer than 200 electrons). From applications to similarly sized PAHs,[15] this CI space appears to be sufficient for ensuring the convergence of the computed excitation energies within accuracies of 0.02 eV with regard to extensions to larger manifolds.

We have to mention that, in this work, we did not investigate the effects of basis-set extensions but we have used the largest workable basis sets (and the highest level of theory) on our hardware set up. On the other hand, according to our previous results[15] the 3-21G and 6-31G results are quite similar while the STO-3G results seem to be less reliable. It is worth recalling that so far none of the currently implemented exchange-correlation functionals is suited for quantitative studies of electronic excitation processes and responses in very large conjugated systems because these potentials decay too fast at large distances.[78,79] In line with greatly underestimated ionization and electron attachment energies, these functionals are indeed known to produce too low electronic excitation energies in large conjugated systems[80] and lead therefore to much too large polarizabilities. Note that, compared with an ab initio treatment of electron correlation, such as second-order Møller–Plesset (MP2) theory, CPHF is also known to overestimate, systematically and rather significantly (by up to 35%), the longitudinal polarizability of extended conjugated chains.[81] At this stage, we would simply like to recall that the main purpose of our work was to identify trends in the aromatic versus the metallic characters of hollow and gigantic PAHs using methods that are qualitatively robust enough to evaluate their magnetic shielding constants and electric polarizabilities.

## Results and Discussion

**Structures**: The compounds studied in this work are displayed in Figure 1. To easily distinguish the hollow hexagonal structures, we resort to a combination of two numbers (***XY***). The first one (***X***) describes the number of benzenoid rings per edge at the external periphery and the second one (***Y***) refers to the number of concentric hexagonal layers of benzenoid rings. If the second number is replaced by **F**, the PAH of interest is full, that is, it has no central hole (and the central benzenoid ring counts for one hexagonal layer). For example **52** is a hexagonal PAH with six edges exhibiting five benzenoid rings, of which two are corner rings, and is a double-layered doughnut.

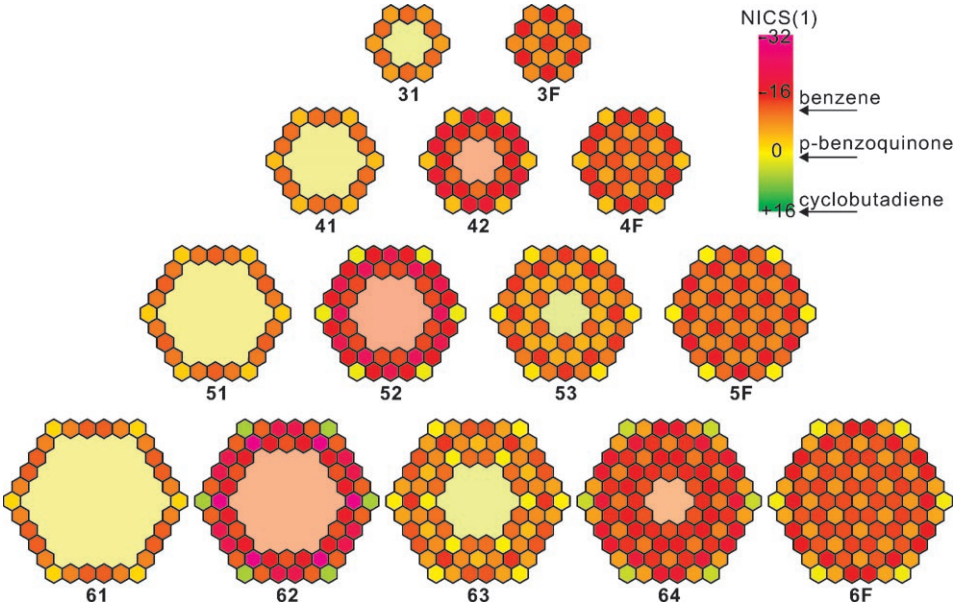


Figure 1. Hexagon structures of the PAHs investigated. Rings are colored in accord with B3LYP/6-31G NICS(1) values.

Most of the molecules investigated have the expected $D_{6h}$ symmetry. Compound **42** has $D_{3h}$ symmetry at the RHF/6-31G level of theory. It has to be mentioned that, with both structures of $D_{3h}$ and $D_{6h}$ symmetry, the RHF wavefunction of compound **42** is not an electronically stable one. Under the constraint of $D_{6h}$ symmetry the most stable UHF/6-31G wavefunction lies 232 kcal mol$^{-1}$ below the RHF/6-31G wavefunction. However, with a $<S^2>$ value of 12.45, the UHF/6-31G wavefunction has extremely high spin contamination. These observations for compound **42** quantitatively call into question the quality of both RHF and UHF calculations in this particular case because the RHF results relate to an excited state and the UHF calculations are physically meaningless. These methodological problems clearly reflect already strong multireference effects in the ground-state wavefunction of compound **42**, and thus the extreme propensity of this compound to undergo electronic excitation and/or symmetry-lowering, which are rather typical features

  

of large metallic systems. In contrast, the closed-shell wavefunction of **42** is electronically stable at the B3LYP/6-31G level of theory as a CIS-type stability calculation based upon this wavefunction shows.

The **62**, **63**, and **64** $D_{6h}$ species are saddle-points on both the HF/6-31G and B3LYP/6-31G potential energy surfaces. Upon symmetry-lowering they relax into bowl-shaped $C_{6v}$ structures at both levels (these $C_{6v}$ structures are referred to as **62b**, **63b**, and **64b**, respectively). In addition to this, it was found that the planar $D_{6h}$ form of **64** has two imaginary frequencies at the HF/6-31G level of theory. The less negative one leads to the $C_{6v}$ **64b** structure and the larger negative one represents a distortion from $D_{6h}$ to $D_{3h}$ symmetry, similarly to the HF/6-31G results obtained for **42**. The $C_{6v}$ form of **64** is also a saddle-point at the HF/6-31G level.

The energy differences between the planar and bowl-shaped compounds are marginal (0.11, 0.32, and 0.08 kcal $mol^{-1}$ at the HF/6-31G level of theory for **62**, **63**, and **64**, respectively, and even less at the B3LYP/6-31G level), so in practice these compounds can be regarded as planar.

**Magnetic properties**: The NICS values at the HF/6-31G//CNDO and B3LYP/6-31G levels of theory are collected in Table 1 and Table 2, respectively (also see Figure 1). The corresponding ring numbers are given in Figure 2. For comparison purposes, NICS(1) values computed for [18]–[66]annulenes at these levels are given in Table 3. The B3LYP and HF results are qualitatively the same except for the annulene rings of $D_{3h}$ symmetry. For these rings, while at the B3LYP level aromaticity smoothly fades away with increas-

Table 1. NICS(1)[a] values for benzene (**BZ**) and compounds **31**–**6F** calculated at the GIAO-HF/6-31G//CNDO level of theory.

| | 1 | 2 | 3 | 4 | 5 | 6 | 7 | 8 | 9 | 10 | 11 | 12 |
|---|---|---|---|---|---|---|---|---|---|---|---|---|
| **BZ** | −12.1 | | | | | | | | | | | |
| **31** | 3.6 | | −7.1 | −12.8 | | | | | | | | |
| **3F** | −17.5 | −7.7 | −8.3 | −17.5 | | | | | | | | |
| **41** | 1.9 | | | | −4.2 | −12.3 | | | | | | |
| **42** | −15.6 | | −19.5 | −13.1 | −3.3 | −20.7 | | | | | | |
| **4F** | −5.6 | −15.4 | −14.1 | −5.0 | −2.9 | −16.0 | | | | | | |
| **51** | 1.1 | | | | | | −2.7 | −11.0 | −14.0 | | | |
| **52** | −16.6 | | | | −30.9 | −17.7 | 3.3 | −18.9 | −23.4 | | | |
| **53** | 6.5 | | −4.5 | −13.8 | −16.4 | −4.9 | −0.5 | −10.2 | −16.4 | | | |
| **5F** | −19.7 | −9.4 | −9.8 | −19.5 | −18.7 | −7.8 | 1.3 | −11.0 | −19.0 | | | |
| **61** | 0.7 | | | | | | | | | −1.9 | −9.7 | −13.9 |
| **62** | −16.2 | | | | | | −41.1 | −22.8 | −17.7 | 9.4 | −13.8 | −27.0 |
| **63** | 4.0 | | | | 1.3 | −12.3 | −16.6 | −8.9 | −3.6 | 0.3 | −6.2 | −14.6 |
| **64** | −16.4 | | −21.8 | −18.1 | −11.6 | −22.5 | −22.7 | −17.0 | −9.4 | 6.5 | −5.6 | −20.1 |
| **6F** | −7.0 | −17.0 | −16.3 | −6.7 | −6.1 | −17.1 | −19.1 | −13.4 | −5.3 | 2.0 | −5.3 | −17.1 |

[a] NICS values were calculated 1 Å above the plane of the molecule. The NICS(1) values are large negative values for aromatic systems, large positive values for antiaromatic systems, and around zero for nonaromatic systems. The corresponding ring numbers are given in Figure 2.

Table 2. NICS(1)[a] values for benzene (**BZ**) and compounds **31**–**6F** calculated at the GIAO-B3LYP/6-31G level of theory.

| | 1 | 2 | 3 | 4 | 5 | 6 | 7 | 8 | 9 | 10 | 11 | 12 |
|---|---|---|---|---|---|---|---|---|---|---|---|---|
| **BZ** | −10.4 | | | | | | | | | | | |
| **31** | 2.7 | | −6.8 | −11.4 | | | | | | | | |
| **3F** | −14.7 | −7.6 | −8.3 | −16.1 | | | | | | | | |
| **41** | 1.6 | | | | −4.3 | −11.1 | | | | | | |
| **42** | −11.6 | | −16.4 | −11.0 | −4.1 | −18.6 | | | | | | |
| **4F** | −6.2 | −13.2 | −13.0 | −6.0 | −3.7 | −15.2 | | | | | | |
| **51** | 1.0 | | | | | | −2.9 | −10.1 | −12.2 | | | |
| **52** | −11.9 | | | | −24.5 | −13.8 | 1.3 | −16.6 | −22.4 | | | |
| **53** | 4.4 | | −4.9 | −12.4 | −14.8 | −5.5 | −1.1 | −10.0 | −14.7 | | | |
| **5F** | −15.6 | −9.0 | −9.4 | −15.9 | −16.8 | −8.4 | 0.2 | −11.2 | −17.7 | | | |
| **61** | 0.7 | | | | | | | | | −2.1 | −9.3 | −12.3 |
| **62** | −11.1 | | | | | | −31.3 | −17.3 | −13.2 | 6.0 | −12.0 | −22.2 |
| **62b**[b] | −11.1 | | | | | | −30.4 | −16.6 | −12.6 | 6.6 | −11.2 | −21.4 |
| **62b**[c] | −11.2 | | | | | | −32.1 | −18.0 | −13.8 | 5.2 | −12.8 | −22.9 |
| **63** | 3.1 | | | | 0.4 | −11.1 | −14.7 | −8.3 | −4.5 | −0.3 | −6.4 | −12.8 |
| **63b**[b] | 3.2 | | | | 0.7 | −10.9 | −14.4 | −8.1 | −4.4 | −0.2 | −6.3 | −12.6 |
| **63b**[c] | 2.9 | | | | 0.2 | −11.3 | −14.9 | −8.5 | −4.7 | −0.4 | −6.7 | −13.0 |
| **64** | −10.1 | | −15.2 | −13.2 | −10.3 | −16.5 | −19.3 | −14.9 | −9.4 | 4.1 | −6.7 | −18.2 |
| **64b**[b] | −9.8 | | −14.8 | −12.8 | −9.2 | −16.1 | −19.0 | −14.6 | −9.1 | 4.3 | −6.5 | −17.9 |
| **64b**[c] | −10.4 | | −15.7 | −13.6 | −10.6 | −16.9 | −19.7 | −15.3 | −9.7 | 3.8 | −7.1 | −18.5 |
| **6F** | −7.4 | −13.6 | −13.4 | −7.3 | −7.2 | −14.2 | −17.2 | −12.8 | −7.0 | 1.0 | −6.3 | −16.0 |

[a] NICS values were calculated 1 Å above the plane of the molecule. The NICS(1) values are large negative values for aromatic systems, large positive values for antiaromatic systems, and around zero for nonaromatic systems. The corresponding ring numbers are given in Figure 2. [b] NICS(1) values from the convex side. [c] NICS(1) values from the concave side.

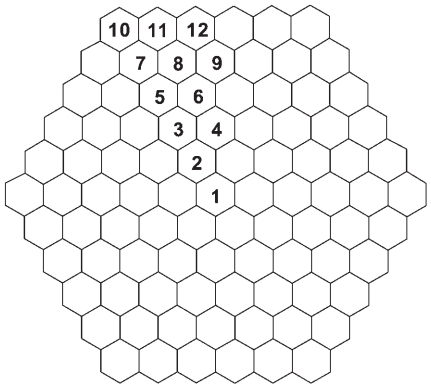


Figure 2. Ring numbering for NICS and Bird index calculations.

ing ring size, nonaromaticity is found at the HF/6-31G level. The origin of this feature lies in the differences in the geometries at the B3LYP and HF/CNDO levels. At the B3LYP level the single–double bond equalization is much more pronounced than at the HF and CNDO levels of theory. It is indeed well-known that theoretical approaches that lack electron correlation tend to systematically overestimate the extent of bond-length alternations in extended π-conjugated chains[71,82–85] to prevent a closure of the HOMO–LUMO gap and near-energy degeneracies therefore.

$^1$H NMR chemical shifts ($\delta$) for the PAHs shown in Figure 1 are collected in Table 4, along with those found for [18]–[66]annulenes. In hollow PAHs, the hydrogen atoms are numbered from the "corner" *Z* configuration double bonds ($\delta_1$, $\delta_2$ …) and the hydrogen atoms in the cavity have a "C" in the index ($\delta_{C1}$, $\delta_{C2}$ …) (see Figure 3). According to a linear regression of data for 80 organic molecules, the RMS and largest deviations from experimental $^1$H NMR chemical shifts at the B3LYP/6-311++G**//B3LYP/6-31+G* level of theory are found to be 0.15 and 0.4 ppm, respectively.[86] Another study on a smaller range of organic compounds, namely on 10 small PAHs (substituted and unsubstituted), shows that the RMS and largest deviations between experimental and B3LYP/6-31G**//B3LYP/6-31G*-calculated chemical shifts are equal to 0.065 and 0.171 ppm, respectively.[87] Our $^1$H NMR shifts, being obtained at a slightly lower level of theory (B3LYP/6-31G) and without any parametric corrections, are certainly a little less accurate. Except for kekulene (**31**) and [18]annulene, there are no available experimental results to compare with. The experimental $\delta_1$, $\delta_2$, and $\delta_{C1}$ chemical shifts reported for kekulene are 7.94, 8.37, and 10.45 ppm, respectively,[88] which is in very reasonable agreement with our B3LYP/6-31G results (7.9, 8.2, and 10.0 ppm, respectively, that is, ~0.5 ppm accuracy). The experimental $^1$H NMR spectra of [18]annulene[89] is a little more complicated because it was found to be strongly dependent upon temperature. At high temperatures (over 314 K) [18]annulene has magnetically equivalent hydrogen atoms because the molecule turns inside out and can

Table 4. $^1$H NMR shifts ($\delta$)[a] for compounds **31**–**6F** and [18]–[66]annulenes calculated at the B3LYP/6-31G level of theory.

| | Symmetry | $\delta_1$ | $\delta_2$ | $\delta_3$ | $\delta_{C1}$ | $\delta_{C2}$ | $\delta_{C3}$ |
|---|---|---|---|---|---|---|---|
| **31** | $D_{6h}$ | 7.9 | 8.2 | | 10.0 | | |
| **3F** | $D_{6h}$ | 9.9 | 10.5 | | | | |
| **41** | $D_{6h}$ | 7.5 | 8.1 | | 9.3 | | |
| **42** | $D_{6h}$ | 12.2 | 14.1 | | −7.4 | | |
| **4F** | $D_{6h}$ | 10.7 | 12.1 | | | | |
| **51** | $D_{6h}$ | 7.3 | 7.9 | 8.3 | 9.2 | 8.7 | |
| **52** | $D_{6h}$ | 13.7 | 16.5 | 17.7 | −9.4 | | |
| **53** | $D_{6h}$ | 9.7 | 10.9 | 11.5 | 12.5 | | |
| **5F** | $D_{6h}$ | 11.3 | 13.1 | 14.1 | | | |
| **61** | $D_{6h}$ | 7.2 | 7.8 | 8.4 | 9.1 | 8.7 | |
| **62/62b** | $D_{6h}/C_{6v}$ | 14.6 | 17.9 | 20.0 | −10.2 | −9.9 | |
| **63/63b** | $D_{6h}/C_{6v}$ | 9.1 | 10.1 | 11.0 | 12.3 | | |
| **64/64b** | $D_{6h}/C_{6v}$ | 12.6 | 15.2 | 17.1 | −4.9 | | |
| **6F** | $D_{6h}$ | 11.6 | 13.7 | 15.3 | | | |
| [18] | $D_{6h}$ | 10.3 | | | −9.3 | | |
| [30] | $D_{3h}$ | 13.0 | 13.9 | | −12.5 | | |
| [30] | $D_{6h}$ | 14.5 | 15.6 | | −16.8 | | |
| [42] | $D_{3h}$ | 10.8 | 11.7 | | −4.8 | −4.6 | |
| [42] | $D_{6h}$ | 19.1 | 20.9 | | −24.2 | −22.8 | |
| [54] | $D_{3h}$ | 9.1 | 9.7 | 9.8 | −0.1 | 0.0 | |
| [54] | $D_{6h}$ | 23.8 | 26.4 | 26.7 | −31.7 | −29.3 | |
| [66] | $D_{3h}$ | 7.8 | 8.2 | 8.4 | 2.9 | 2.7 | 2.7 |
| [66] | $D_{6h}$ | 28.5 | 31.8 | 32.5 | −39.2 | −35.9 | −35.4 |

[a] Chemical shifts are given in ppm. We assumed that the calculated gas-phase absolute isotropic magnetic shielding of hydrogen atoms in $CH_4$ is equal to the solvent-phase experimental $^1$H NMR chemical shift of $CH_4$. The corresponding atom numbers are given in Figure 3.

Table 3. NICS(1)[a] values for benzene (**BZ**) and [18]–[66]annulenes calculated at the GIAO-HF/6-31G//CNDO, GIAO-HF/6-31G, and GIAO-B3LYP/6-31G levels of theory.

| | **BZ** | [18] | [30] | [30] | [42] | [42] | [54] | [54] | [66] | [66] |
|---|---|---|---|---|---|---|---|---|---|---|
| symmetry | $D_{6h}$ | $D_{6h}$ | $D_{3h}$ | $D_{6h}$ | $D_{3h}$ | $D_{6h}$ | $D_{3h}$ | $D_{6h}$ | $D_{3h}$ | $D_{6h}$ |
| HF/6-31G//CNDO | −12.1 | −13.3 | 0.1 | −15.7 | 0.3 | −16.5 | 0.2 | −16.9 | 0.1 | −17.1 |
| HF/6-31G | −12.0 | −12.9 | 0.4 | −15.3 | 0.3 | −16.2 | 0.2 | −16.6 | 0.1 | −16.8 |
| B3LYP/6-31G | −10.4 | −11.9 | −11.2 | −13.9 | −5.3 | −14.6 | −2.5 | −15.0 | −1.1 | −15.2 |

[a] NICS values were calculated 1 Å above the plane of the molecule. The NICS(1) values are large negative values for aromatic systems, large positive values for antiaromatic systems, and around zero for nonaromatic systems.

  

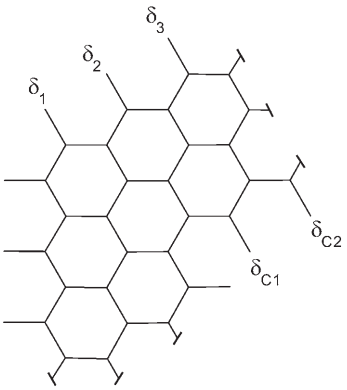


Figure 3. Hydrogen atom numbering for chemical shift calculations.

take up three isodynamic conformations. Below the coalescence temperature of 314 K, [18]annulene no longer turns inside out and, accordingly, the $^1$H NMR spectrum of [18]annulene splits into two peaks, the separation of which increases linearly with decreasing temperature. In reference [89], the temperature dependence below 314 K was explained in terms of vibrational distortions, which tend to reduce the ring current at higher temperatures. The $\delta_1$ and $\delta_{C1}$ chemical shifts of [18]annulene extrapolated to 0 K from the experimental data are 10.28 and −5.38 ppm, compared with theoretical (B3LYP/6-31G) values of 10.3 and −9.3 ppm, respectively. With regard to the excellent agreement described above between the B3LYP/6-31G and experimental $^1$H NMR chemical shifts of a rigid system like kekulene, the much larger difference (4 ppm) between the calculated and measured $\delta_{C1}$ chemical shifts could be tentatively ascribed to the consequences of residual vibrations at 0 K, which were discarded from our calculations of chemical shifts for fixed molecular geometries that correspond to global energy minima. Indeed, the much stronger temperature dependence that has been observed experimentally for the $\delta_{C1}$ chemical shifts make us believe that, in a conformationally highly flexible system like [18]annulene, zero-point vibrations should have a larger extent and thus a larger impact on the chemical shifts of hydrogen atoms inside the cavity (in plots of the experimentally measured chemical shifts versus temperature, slopes of −0.70 and −0.29 were reported for the $\delta_{C1}$ and $\delta_1$ shifts, respectively).

The NICS values of almost all hexagon rings in the PAHs investigated are large negative numbers, which indicate locally high aromaticity. The only exceptions are the "corner" hexagon rings with small negative or positive NICS values indicating weakly aromatic or nonaromatic benzenoid rings. The NICS values of the central hole of the **31**, **41**, **51**, and **61** singly layered and **53**, **63**, and **63b** triply layered PAH doughnuts are small and positive, which implies that for these compounds an external magnetic field will result in an overall marginally small and paratropic circular current around the central hole. It has been shown in detailed computations of π ring currents that, for coronene[90] and kekulene,[91] such a small current is the global result of two circular currents, one diatropic, the other paratropic, that rotate therefore in opposite directions around the concentric annulene ring located around the central hole.[92,93] Most certainly the same compensation of partial currents applies here for odd-layered doughnut species which contain an even (two or four) number of concentric "annulenoid" rings. Inversely, it is then logical to assume that, in even-layered doughnut species with, thus, an odd number of concentric "annulenoid" rings, the partial paratropic ring currents will not fully compensate the diatropic ones. For these systems, a large diatropic current around the central hole is thus globally expected.[44,94]

Indeed, large negative NICS values characterize the central hole of even-layered doughnuts such as compounds **42**, **52**, **62**, **62b**, **64**, and **64b** and foretell the induction of an overall extremely strong and diatropic circular current around the central hole in the presence of an external magnetic field. The extreme shielding of the external magnetic field inside the cavity is in this case also supported by the large negative chemical shifts of the hydrogen atoms in the cavity. In a broader sense it is reasonable to state that even-layered "doughnut" PAHs have strongly aromatic central holes whereas odd-layered "doughnuts" have nonaromatic central holes. By the same logic, compounds **3F** and **5F** can also be regarded as even-layered PAHs with, at their center, an exceptionally strongly aromatic central hole, which is surrounded by lesser aromatic benzenoid rings. Similarly, and in line with the above classification, compounds **4F** and **6F** can be described as odd-layered PAHs with, at their center, a benzenoid hole characterized by NICS(1) indices (−6.2 and −7.4) that are indicative of reduced aromaticity compared with benzene (−10.4) at the same (B3LYP/6-31G) level of theory. Based on NICS(1) values the aromaticity in the outer layer hexagon rings always increases from the "corner" ring to the rings at the centers of the "polyacene" edges. Inversely, in the next layer towards the central hole aromaticity locally decreases from the corner rings to the centers of the edges. When we pass to the next layer towards the central hole, this tendency reverses again, and so on in the following layers. The changes in the chemical shifts of outer hydrogen atoms within a molecule are in good accord with the NICS(1) values [a larger $\delta_1$ chemical shift is observed if the corresponding hydrogen atom is connected to a ring with a larger NICS(1) value]. This is not true, however, for the hydrogen atoms in the central hole. The differences between the NICS(1) values for the concave and convex sides of the bowl-shaped compounds (**62b**, **63b**, and **64b**) relative to the planar form **64**, systematically indicates an increase in the π-electron density on the concave side and quite naturally, therefore, a lowering of the π-electron density inside the bowl.

The differences observed in the local aromaticity of the central holes of even- and odd-layered PAH doughnuts can be rationalized according to Kekulé structures. The structure of PAH doughnuts can be discussed in terms of three basic types of Kekulé bonding patterns, namely the pure benzenoid (Figure 4f and 4g), pure annulenoid (Figure 4a–c), and

  

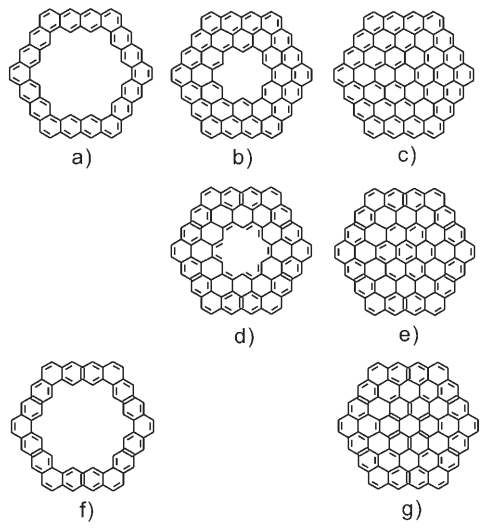


Figure 4. Some Kekulé structures of selected PAHs.

mixed benzenoid–annulenoid (Figure 4d and 4e) types. We calculated the energies of the Kekulé structures shown in Figure 4 by using the NBO[95] localization technique and the B3LYP/6-31G geometries. During the NBO localization the NBO orbitals of the desired molecule were first calculated assuming a nonlocalized structure. In the next step all electrons from the non-Lewis (Rydberg and antibonding) orbitals were deleted (using the NOSTAR keyword) from the NBO basis set in order to obtain a bonding structure with only pure single and double bonds that are characterized by occupation numbers equal to 2.0 and 4.0, respectively (localized structure). In the final step we used these electron densities to evaluate the energy of the localized system. The energy difference between the localized and nonlocalized structures defines the NBO localization energy. The most stable structures are the pure benzenoid structures while the least stable ones are purely annulenoid. The energies of the mixed structures lie between those of the purely annulenoid and benzenoid structures. The compounds sketched in Figure 4 clearly possess numerous other Kekulé structures but the energy differences between the benzenoid and annulenoid structures are sufficiently enlightening that we did not deem it necessary to consider too many varieties. Specifically, the energy differences between the annulenoid and benzenoid structures shown in Figure 4a and 4f and between 4c and 4g are around 180 and 130 kcal mol$^{-1}$, respectively. The resonance (nonlocalized) bonding pattern is a linear combination of Kekulé structures in which the most stable Kekulé structures dominate and it is rather clear that the bonding pattern for the odd-layered doughnuts will be the benzenoid one (thus 4f and 4g for compounds **41** and **4F** displayed in Figure 4). However, in the case of even-layered PAHs (compounds **42**, **52**, **62**, **62b**, **64**, and **64b**), it is clear that no pure benzenoid structure can exist (see, for example, Figure 4b and 4d). In Figure 4d, the internal layer of compound **42** remains in the annulenoid form, which clearly should be more stable than any alternative radical Kekulé structure.

We also investigated the $S_0$–$S_1$ excitation energies of the PAHs studied and compared them with those of annulenes (Table 5).[96] We used the CIS-ZINDO-S//CNDO level of theory as described in our previous study and the results for compounds **31**–**53** are also taken from this previous work.[15] The $S_0$–$S_1$ excitation energies normally progressively decrease with increasing system size but here the even-layered PAH doughnuts with strongly aromatic central holes (**42**, **52**, **62**, and **64**) have much lower HF and B3LYP HOMO–LUMO gaps, and correspondingly also much lower CIS-ZINDO-S//CNDO excitation energies, than other PAHs. Note that the HOMO–LUMO gap has often been used as an important criteria for characterizing PAH compounds and unravelling their ring current (diamagnetic/paramagnetic) properties.[27,40–44,46,97–99] We also found in a previous study that the correlation between reactivity indices and HOMO–LUMO gaps, along with $S_0$–$S_1$ excitation energies, is quite good in this class of compounds.[100] In addition, the $S_0$–$S_1$ excitation energies of PAH doughnuts with strongly aromatic central holes (**42**, **52**, **62**, and **64)** are similar to the $S_0$–$S_1$ excitation energies of the aromatic ($D_{6h}$) annulene compounds with a central hole of equal size. Conversely, the $S_0$–$S_1$ excitation energies of PAH doughnuts having no aromatic central holes (**41**, **51**, **61**, and **63**) are comparable to the $S_0$–$S_1$ excitation energies of nonaromatic ($D_{3h}$) annulene compounds with a central hole of equal size. We would like to emphasize the fact that even-layered hollow PAHs with magnetically aromatic central holes have lower $S_0$–$S_1$ excitation energies than the odd-layered PAHs with magnetically nonaromatic or weakly aromatic central holes. This evident-

Table 5. $S_0$–$S_1$[a] transitions and HOMO–LUMO band gaps for compounds **31**–**6F** and [18]–[66]annulenes.

| Compound | [18] | [30] | [30] | [42] | [42] | [54] | [54] | [66] | [66] | |
|---|---|---|---|---|---|---|---|---|---|---|
| symmetry | $D_{6h}$ | $D_{6h}$ | $D_{3h}$ | $D_{6h}$ | $D_{3h}$ | $D_{6h}$ | $D_{3h}$ | $D_{6h}$ | $D_{3h}$ | |
| $S_0$–$S_1$ trans. | 1.46 | 0.72 | 2.16 | 0.39 | 2.17 | 0.20 | 2.19 | 0.08 | 2.28 | |
| HF band gap[b] | 6.24 | 4.26 | 7.50 | 3.26 | 7.22 | 2.66 | 7.08 | 2.25 | 7.01 | |
| B3 band gap[c] | 2.76 | 1.80 | 1.88 | 1.34 | 1.65 | 1.07 | 1.51 | 0.89 | 1.42 | |
| Compound | **31** | **41** | **42** | **51** | **52** | **53** | **61** | **62** | **63** | **64** |
| $S_0$–$S_1$ trans. | 3.02 | 2.87 | 1.02 | 2.75 | 0.57 | 2.00 | 2.61 | 0.34 | 1.87 | 0.83 |
| HF band gap[b] | 8.54 | 7.97 | 4.16 | 7.29 | 3.04 | 5.64 | 6.68 | 2.40 | 5.29 | 3.10 |
| B3 band gap[c] | 3.60 | 3.10 | 1.64 | 2.59 | 1.14 | 1.92 | 2.16 | 0.84 | 1.64 | 1.06 |

[a] $S_0$–$S_1$ transitions given in eV calculated at the CIS-ZINDO-S//CNDO level of theory. [b] The HF band gap measured in eV is the HOMO–LUMO gap calculated at the HF/6-31G level. [c] The B3 band gap measured in eV is the HOMO–LUMO gap calculated at the B3LYP/6-31G level.

  

ly reflects a very natural correlation between the strength of the response to an external magnetic field in terms of ring currents and the propensity of electrons to undergo excitations into low-lying unoccupied levels.

**Geometry**: The *XYZ* coordinates of the structures can be found in the Supporting information. Here we discuss only the results of the B3LYP/6-31G calculations. All the calculated C–C bond lengths in compounds **31**–**6F** are between 1.36 and 1.48 Å. The difference in C–C bond length between planar and the corresponding bowl-shaped compounds (**62**, **62b**, **63**, **63b**, **64**, and **64b**) is typically almost negligible, being around 0.001 Å. The longest C–C bonds in a given molecule are the inner "corner" bonds and the shortest ones are the outer "corner" bonds. The majority of C–C bond lengths are around 1.42–1.43 Å and closer to this value if the bond is farther from the edge of the molecule. We compared the bond lengths in the PAHs investigated with similar systems. The C–C bond length in benzene (1.401 Å) is slightly shorter than the majority of C–C bonds in the PAHs investigated. We also calculated the C–C bond lengths in infinite-sized alternating-double-bond all-(*E*)-alkenes. In these structures two different C–C bond lengths exist, a shorter one of 1.374 Å and a longer one of 1.427 Å. These values were obtained by extrapolating from the bond lengths around the middle of the $C_{12n+6}H_{12n+8}$ ($n=0$, 1, 2, 3, 4, and 5) series of alternating-double-bond all-(*E*)-alkenes (see Scheme 1). We also investigated the C–C bond lengths

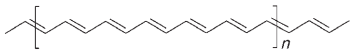

Scheme 1. Alternating-double-bond all-(*E*)-alkenes used for CH unit energy and C–C bond length extrapolations ($n=0$–5).

in [18]-, [30]-, [42]-, [54]-, and [66]annulenes but analysis is a little more complicated because the large annulenes have $D_{3h}$ geometry while [18]annulene has $D_{6h}$ symmetry. We calculated both $D_{3h}$ and $D_{6h}$ geometries for the larger annulenes. In the case of $D_{6h}$ structures the bond lengths are similar to those in benzene. The shortest bond length in [66]annulene is 1.399 Å and the longest one is 1.406 Å and with increasing size of species the bond lengths get closer to these values. The longest bonds are the "corner" bonds (*Z* configuration). In the case of the $D_{3h}$ annulenes the longest and shortest bond lengths seem to converge to 1.436 and 1.374 Å. These values are similar to the extrapolated bond lengths in the infinite-sized alternating-double-bond all-(*E*)-alkenes (Scheme 1), showing clearly the nonaromatic nature of the $D_{3h}$ annulenes. The majority of C–C bond lengths in compounds **31**–**6F** are relatively long compared with other highly aromatic systems, but are rather equalized. The extent of alternation of C–C bond lengths rapidly decreases with increasing distance from the "corner" bonds. Note that the inner shape of the central hole in molecules **31**–**64** is much more similar to $D_{6h}$ annulenes than the outer shape (long and short "corner" bonds). It is clear that the presence of large aromatic circuits has no confirmable effect on geometry.

We also calculated the Bird indices[51] of the individual rings in compounds **31**–**6F** based on Gordy's bond orders.[101] Gordy's bond order is calculated by using a simple inverse square relation of the form $N=aR^{-2}+b$, where $N$ is the Gordy's bond order and $R$ is the bond length. Values of $a$ and $b$ were calculated from the bond lengths of ethane and ethene for which we assumed that Gordy's bond orders are $N=1$ and $N=2$, respectively. Bird indices are normalized on a scale of 0–100 and measure the standard deviations of bond lengths or bond orders in a given ring. The two extrema of Bird indices relate to two reference situations, namely a ring with fully equalized bond lengths or bond orders (Bird index = 100) or a ring exhibiting a fully localized π-bonding pattern, that is, a perfect alternation of single C–C and double C=C bonds (Bird index = 0). The reference single and double bonds were the B3LYP/6-31G-calculated C–C bonds in ethane and ethene, respectively. In addition to this we also calculated the Bird indices for larger concentric ring circuits with 18, 30, 42, 54, and 66 carbon atoms within the molecules (annulene indices $A_{18}$–$A_{66}$) because some PAHs were expected to show a more pronounced annulenoid nature. The results are collected in Table 6 and the corresponding ring numbers are given in Figure 2. For comparison we also calculated the Bird indices for annulenes. The $D_{6h}$ annulenes have high Bird indices (93, 96, 97, 98, and 98 for [18]-, [30]-, [42]-, [54]-, and [66]annulenes, respectively) while $D_{3h}$ annulenes have lower Bird indices (85, 76, 74, and 74 for [30]-, [42]-, [54]-, and [66]annulenes, respectively). The infinite-sized annulene would have a Bird index of 74, in view of the extrapolated C–C bond lengths in the infinite-sized alternating-double-bond all-(*E*)-alkenes (Scheme 1). The rationale for this extrapolation is that the bond lengths in a suitable large nonaromatic ($D_{3h}$ symmetry) annulene far away from the *Z* configuration "corner" bonds are similar to the bond lengths in the infinite-sized alternating-double-bond all-(*E*)-alkenes. Based on the latter findings all rings having a Bird index of around 70 or less might not be aromatic despite high bond equalization. In addition to this the Bird index of a nonaromatic ring surrounded by condensed aromatic rings may be higher than expected and, furthermore, the Bird index cannot differentiate benzene from more aromatic systems. By analyzing the Bird and annulene indices we can conclude that the PAHs investigated are overall aromatic and the rings farther from the edges and "corners" are more aromatic. The "corner" rings and the central holes may not be aromatic. It is not easy to compare the overall aromaticity of PAH systems of different size using the Bird (and other similar geometry-based) indices but it is rather clear that the larger the extent of the central hole, the lower the global aromaticity of the studied system from a geometric view point since a larger central hole involves more edge and fewer aromatic rings. In the case of compounds **31**–**6F** the Bird indices do not correlate well with the local magnetic criteria of aromaticity such as the NICS(1) indices, except for the outer-layer rings

  

Table 6. Bird[a] and annulene[b] indices for compounds **31**–**6F**.

| | 1 | 2 | 3 | 4 | 5 | 6 | 7 | 8 | 9 | 10 | 11 | 12 | $A_{18}$ | $A_{30}$ | $A_{42}$ | $A_{54}$ | $A_{66}$ |
|---|---|---|---|---|---|---|---|---|---|---|---|---|---|---|---|---|---|
| **31** | 70 | | 67 | 85 | | | | | | | | | 70 | 70 | | | |
| **3F** | 100 | 96 | 73 | 87 | | | | | | | | | 97 | 72 | | | |
| **41** | 71 | | | | 62 | 78 | | | | | | | | 71 | 70 | | |
| **42** | 73 | | 90 | 84 | 70 | 85 | | | | | | | 73 | 99 | 74 | | |
| **4F** | 100 | 98 | 96 | 98 | 68 | 84 | | | | | | | 97 | 99 | 72 | | |
| **51** | 72 | | | | | | 59 | 65 | 78 | | | | | | 72 | 72 | |
| **52** | 74 | | | | 87 | 83 | 67 | 83 | 86 | | | | | 74 | 97 | 74 | |
| **53** | 71 | | 88 | 86 | 97 | 95 | 66 | 80 | 88 | | | | 71 | 95 | 96 | 72 | |
| **5F** | 100 | 98 | 98 | 99 | 96 | 97 | 66 | 81 | 87 | | | | 99 | 97 | 98 | 72 | |
| **61** | 73 | | | | | | | | | 58 | 69 | 75 | | | | 73 | 73 |
| **62** | 74 | | | | | | 84 | 80 | 84 | 66 | 80 | 84 | | | 74 | 98 | 75 |
| **62b** | 74 | | | | | | 84 | 80 | 84 | 66 | 81 | 84 | | | 74 | 97 | 76 |
| **63** | 77 | | | | 88 | 84 | 94 | 94 | 95 | 64 | 78 | 86 | | 77 | 96 | 94 | 73 |
| **63b** | 72 | | | | 87 | 84 | 94 | 94 | 95 | 64 | 77 | 85 | | 72 | 96 | 94 | 73 |
| **64** | 73 | | 90 | 86 | 98 | 97 | 94 | 97 | 96 | 65 | 79 | 86 | 73 | 99 | 98 | 96 | 74 |
| **64b** | 72 | | 89 | 85 | 98 | 98 | 94 | 97 | 96 | 65 | 79 | 86 | 72 | 99 | 98 | 96 | 74 |
| **6F** | 100 | 99 | 99 | 100 | 98 | 98 | 94 | 96 | 96 | 65 | 78 | 85 | 99 | 100 | 97 | 96 | 73 |

[a] Bird indices were calculated using B3LYP/6-31G geometries. The corresponding ring numbers are given in Figure 2. [b] The $A_{18}$–$A_{66}$ annulene indices were calculated using B3LYP/6-31G geometries.

(see Table 2 and Table 6, especially the "inner corner" rings and their surroundings).

**Aromatic stabilization energies**: There are different ways to calculate aromatic stabilization energies (ASEs). The simplest way to estimate ASEs is through the classical isodesmic bond separation energies (IBSEs).[36] Isodesmic reactions are transformations in which the number of bonds of the same type are preserved. In our case the IBSEs were calculated as the reaction energy (using the calculated total energies) for the hypothetical transformation shown in Equation (1).

$$\begin{aligned} &C_aH_b + (2a-b)CH_4 \\ &\rightarrow (a-b/2)H_3C-CH_3 + (a/2)H_2C=CH_2 \end{aligned} \quad (1)$$

However, IBSEs do not deal with the fact that different hybrid-state carbon atoms have different bonding energies. To cope with this we also calculated the homodesmotic stabilization energies (HSEs).[36] In addition to the requirements associated with isodesmic bond separation reactions, homodesmotic reactions contain on both sides of the reaction the same number of atoms in the same hybrid states. In our case the HSEs were calculated as the reaction energy (using calculated total energies) for the hypothetical transformation shown in Equation (2).

$$\begin{aligned} &C_aH_b + (a/2)H_2C=CH_2 + (2a-2b)CH_3-CH=CH_2 \\ &\rightarrow (a-b)H_2C=C(CH_3)_2 + (a-b/2)H_2C=CH-CH=CH_2 \end{aligned} \quad (2)$$

However, HSEs still partly account for contributions to the energy other than aromaticity, such as the π and σ delocalization energies, the cyclization energy, and ring strains. To further reduce the effect of delocalization in the evaluation of the aromatic stabilization energies we also calculated these from a special homodesmotic reaction in which the product/reactants contain extended delocalized parts. These homodesmotic reactions are often referred to as "super"homodesmotic reactions. In our case, superhomodesmotic stabilization energies (SSEs) were calculated by resorting to a hypothetical fragmentation of PAHs into CH units and carbon atoms, which are assumed to be taken from large, nonaromatic, but highly conjugated systems so that the energies of these fragments explicitly account for the delocalization, π and σ bonding, and other related energies in nonaromatic but highly conjugated systems. In short, such transformations are of the form given in Equation (3).

$$C_aH_b \rightarrow (a-b)C + bCH \quad (3)$$

Specifically, in this work, the energies of the CH fragments were estimated from a hypothetical all-(*E*)-polyacene chain of infinite dimension, that is, by extrapolating to infinite size the B3LYP/6-31G energies obtained for the $C_{12n+6}H_{12n+8}$, ($n=0$, 1, 2, 3, 4, and 5) series of alternating-double-bond all-(*E*)-alkenes (see Scheme 1). To evaluate the energy of a carbon atom linked to three carbon atoms in a large, conjugated, but essentially nonaromatic (quinoidal) molecule, we considered the infinitely large dimethylene-dihydro-polyacene with the two methylenes being located at the β and β′ positions within two different terminating rings (overall $C_{2h}$ symmetry). The energy of an individual carbon atom in an infinite-conjugated and nonaromatic system was extrapolated from the results of B3LYP/6-31G calculations performed on the $C_{8n+12}H_{4n+12}$ ($n=0$–9) series (Scheme 2) and by using the previously calculated energy of the CH fragment. In practice, the SSEs are the reaction energies (using calculated total energies) of the transformations de-

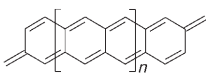


Scheme 2. β,β′-Dimethylene-dihydro-polyacenes used for carbon atom energy extrapolation ($n=0$–9).

  

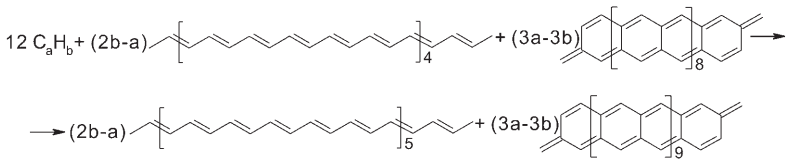


Scheme 3. Transformations used during the calculation of superhomodesmotic stabilization energies.

Table 7. Isodesmic bond (IBSE)[a,b], homodesmotic (HSE)[a,c], and superhomodesmotic (SSE)[a,d] stabilization energies for benzene (**BZ**), compounds **31**–**6F**, and [18]–[66]annulene.

| | Symmetry | C[e] | H[e] | IBSE | HSE | SSE |
|---|---|---|---|---|---|---|
| **BZ** | $D_{6h}$ | 6 | 6 | 67.9 | 22.5 | 16.3 |
| **31** | $D_{6h}$ | 48 | 24 | 84.8 | 17.5 | 9.4 |
| **3F** | $D_{6h}$ | 54 | 18 | 98.4 | 23.8 | 15.0 |
| **41** | $D_{6h}$ | 72 | 36 | 83.7 | 16.4 | 8.3 |
| **42** | $D_{6h}$ | 90 | 30 | 94.4 | 19.8 | 11.1 |
| **4F** | $D_{6h}$ | 96 | 24 | 102.4 | 24.1 | 15.1 |
| **51** | $D_{6h}$ | 96 | 48 | 82.4 | 15.1 | 7.0 |
| **52** | $D_{6h}$ | 126 | 42 | 93.6 | 19.0 | 10.2 |
| **53** | $D_{6h}$ | 144 | 36 | 100.4 | 22.2 | 13.1 |
| **5F** | $D_{6h}$ | 150 | 30 | 104.9 | 24.5 | 15.2 |
| **61** | $D_{6h}$ | 120 | 60 | 81.3 | 14.0 | 5.9 |
| **62**/**62b** | $D_{6h}/C_{6v}$ | 162 | 54 | 92.7 | 18.1 | 9.4 |
| **63**/**63b** | $D_{6h}/C_{6v}$ | 192 | 48 | 99.8 | 21.5 | 12.5 |
| **64**/**64b** | $D_{6h}/C_{6v}$ | 210 | 42 | 103.5 | 23.1 | 13.8 |
| **6F** | $D_{6h}$ | 216 | 36 | 106.7 | 24.8 | 15.4 |
| [18] | $D_{6h}$ | 18 | 18 | 45.6 | 0.2 | −6.0 |
| [30] | $D_{3h}$ | 30 | 30 | 48.1 | 2.6 | −3.5 |
| [30] | $D_{6h}$ | 30 | 30 | 48.1 | 2.6 | −3.5 |
| [42] | $D_{3h}$ | 42 | 42 | 49.0 | 3.6 | −2.5 |
| [42] | $D_{6h}$ | 42 | 42 | 48.8 | 3.4 | −2.8 |
| [54] | $D_{3h}$ | 54 | 54 | 49.6 | 4.2 | −2.0 |
| [54] | $D_{6h}$ | 54 | 54 | 49.2 | 3.8 | −2.4 |
| [66] | $D_{3h}$ | 66 | 66 | 50.0 | 3.6 | −1.6 |
| [66] | $D_{6h}$ | 66 | 66 | 49.5 | 4.1 | −2.1 |

[a] Results of calculations at the B3LYP/6-31G level of theory, given in kcal mol$^{-1}$. All energy values were normalized to six carbon units. [b] IBSE is the heat of the reaction shown in Equation (1). [c] HSE is the heat of the reaction shown in Equation (2). [d] SSE is the heat of the $C_aH_b \rightarrow (a-b)C + bCH$ reaction. See text for details. [e] The numbers of carbon and hydrogen atoms are given in columns C and H.

scribed in Scheme 3. The IBSE, HSE, and SSE values of the PAHs and annulenes investigated at the B3LYP/6-31G level of theory are collected in Table 7. The energy difference between the bowl-shaped and the corresponding planar structures is marginal hence the calculated ASEs are practically the same. The trends within the IBSE, HSE, and SSE are exactly the same, but the absolute values differ. In the case of hollow PAHs the aromaticity progressively decreases with increasing size for series of compounds containing the same number of layers (**31**–**41**–**51**–**61**, **42**–**52**–**62**, and **53**–**63**). In contrast to the magnetic indices of aromaticity, the aromatic stabilization energies of fully condensed PAHs (**3F**–**4F**–**5F**–**6F**) regularly increase with increasing system size. As for the structural criteria, aromaticity from a stability viewpoint also monotonically increases in systems of comparable size but containing an increasing number of layers (**31**–**3F**, **41**–**42**–**4F**, **51**–**52**–**53**–**5F**, and **61**–**62**–**63**–**64**–**6F**). In other words, the larger the central hole in the PAH doughnuts the less stable the system. So this work confirms the statistically multidimensional nature of aromaticity and an inherent dichotomy between the magnetic and energetic/structural indices for it.

Holes in extended PAHs appear to induce locally severe destabilizing effects (IBSE and SSE differences between **64** and **6F** are about 250 and 70 kcal mol$^{-1}$, respectively), which makes us believe that energy destabilization does not just result from an alteration of aromaticity but may also be due to other effects pertaining to the alteration of delocalization patterns of π electrons. In line with this it was interesting to find that the differences between IBSEs, HSEs, and SSEs are smaller for benzene than for larger fused PAH systems with fewer hydrogen atoms relative to carbon atoms. This shows that the energy gain due to π delocalization is higher in the case of carbon atoms with only neighboring carbon atoms than in the case of carbon atoms having one hydrogen neighbor. This view is also supported by the fact that the HSE of a CH fragment from an infinite-sized alternating-double-bond all-(*E*)-alkene is 1.0 kcal mol$^{-1}$ whereas the HSE per carbon atom with only carbons as neighboring atoms in an infinite-sized dimethylene-dihydro-polyacene is 1.7 kcal mol$^{-1}$. The result of ASE analysis of annulenes is in good accord with the concept of conjugated circuits[102] because the ASE is rather small in the case of large conjugated circuits. The fact that annulenes with $D_{3h}$ symmetry are increasingly more stable than those with $D_{6h}$ symmetry with increasing ring size means that extra large conjugated circuits could have an increasing destabilizing effect.[33,55,62] The **42**, **52**, **62**, **62b**, **64**, and **64b** PAHs have mixed benzenoid-annulenoid structures and retain the $C_6$ rotation axes, which is unfavorable for large annulenoid structures because possible symmetry-lowering to a point group with a $C_3$ rotational axis would cause more energy loss in the benzenoid region compared with the energy gain in the annulenoid region. In addition to this the annulenoid parts of the latter compounds are developed around their respective central holes (instead of their outer regions) because in this arrangement the conjugated circuits are minimized, which reduces the overall loss in aromatic stabilization originating from the annulenoid part. The increasing IBSE, HSE, and SSE values within the annulene series can be explained by the smaller ratio of *Z*/*E* double-bond configurations. It is clear that large aromatic circuits do not have any stabilizing effect, but we can still observe the effect of ring currents in large circuits in an external magnetic field.

**Polarizabilities**: In Table 8 we display the principal components of the polarizability tensor and the isotropic polarizability $\{a = (1/3)\mathrm{tr}[\overrightarrow{\alpha}]\}$ obtained from these at the HF/6-31G and B3LYP/6-31G levels for the related geometries. For the sake of structural insight we also provide at these levels of theory the lowest vibrational frequencies.

  

Table 8. Average ring polarizability for compounds **31**–**6F**.

| | | B3LYP/6-31G | | | | HF/6-31G | | | |
|---|---|---|---|---|---|---|---|---|---|
| | π electrons | $\alpha_{xx}$[a] | $\alpha_{zz}$[a] | ISO[b] | LOW[c] | $\alpha_{xx}$[a] | $\alpha_{zz}$[a] | ISO[b] | LOW[c] |
| **31** | 48 | 110.1 | 15.5 | 78.6 | 33 | 92.6 | 15.3 | 66.8 | 35 |
| **3F** | 54 | 113.0 | 14.6 | 80.2 | 41 | 96.1 | 14.4 | 68.9 | 45 |
| **41** | 72 | 136.6 | 15.6 | 96.2 | 18 | 108.2 | 15.3 | 77.3 | 20 |
| **42** | 90 | 161.3 | 14.5 | 112.3 | 14 | 142.3 | 14.3 | 99.6 | *2515i* |
| **4F** | 96 | 137.2 | 14.0 | 96.2 | 24 | 112.1 | 13.8 | 79.3 | 26 |
| **51** | 96 | 165.5 | 15.7 | 115.5 | 11 | 122.9 | 15.4 | 87.1 | 11 |
| **52** | 126 | 223.2 | 14.5 | 153.6 | 4 | 202.9 | 14.3 | 140.1 | *5i* |
| **53** | 144 | 156.9 | 13.9 | 109.2 | 5 | 122.7 | 13.7 | 86.4 | 1 |
| **5F** | 150 | 163.4 | 13.6 | 113.5 | 16 | 129.5 | 13.4 | 90.8 | 18 |
| **61** | 120 | 195.5 | 15.7 | 135.5 | 8 | 135.6 | 15.4 | 95.5 | 6 |
| **62** | 162 | 298.6 | 14.5 | 203.9 | *5i* | 278.5 | 14.3 | 190.4 | *8i* |
| **62b** | 162 | 298.3 | 14.7 | 203.8 | 7 | 277.7 | 14.8 | 190.1 | 11 |
| **63** | 192 | 185.0 | 13.9 | 127.9 | *7i* | 139.1 | 13.7 | 97.3 | *10i* |
| **63b** | 192 | 184.5 | 14.2 | 127.7 | 10 | 138.4 | 14.2 | 97.0 | 12 |
| **64** | 210 | 211.1 | 13.5 | 145.2 | *5i* | 177.6 | 13.3 | 122.8 | *1641i* |
| **64b** | 210 | 211.0 | 13.6 | 145.2 | 6 | 177.1 | 13.5 | 122.6 | *1641i* |
| **6F** | 216 | 191.6 | 13.3 | 132.2 | 12 | 148.9 | 13.2 | 103.6 | 12 |

[a] $\alpha_{xx}$ and $\alpha_{zz}$ are the $XX$ and $ZZ$ components of the average ring polarizability tensor, given in bohr$^3$. Note that $\alpha_{xx}=\alpha_{yy}$. [b] ISO is the isotropic average ring polarizability, given in bohr$^3$. [c] LOW is the lowest harmonic vibrational frequency, given in cm$^{-1}$.

Electric polarizabilities are intrinsically size-extensive properties, that is, they tend to scale proportionally with system size when the system becomes large enough (note that polarizabilities have the dimension of volume). Therefore, to meaningfully compare the polarizabilities of systems of different size, we focused on average ring values. The average polarizabilities per benzenoid ring reported in Table 8 were obtained by multiplying by six the computed electronic polarizabilities and by dividing the obtained result by the number of carbon atoms in the molecule of interest. From Table 8, it is clear that the linear regime is rather quickly reached for the out-of-plane ($\alpha_{zz}$) component of the polarizability tensor, which is quite naturally much smaller than the in-plane components ($\alpha_{xx}=\alpha_{yy}$). The latter components, and therefore the isotropic polarizabilities, tend overall to increase rapidly with system size. However, in straightforward analogy with the observations made previously for the lowest excitation energies, HOMO–LUMO gaps, and magnetic indices of aromaticity, these in-plane and isotropic polarizabilities exhibit systematic and very significant fluctuations. Running through the **31**–**41**–**51**–**61, 3F**–**42**–**52**–**62**, **4F**–**53**–**63, 5F**–**64** series, we note that, in all cases, the average isotropic ring polarizability increases monotonically with system size. It is clear that compounds as large as the **6λ** ($\lambda=$**1**–**4,F**) ones are still too small to observe the linear scaling in size that is normally expected for size-extensive properties. Much larger structures will be necessary to ensure such a scaling. It is also very apparent from Table 8 that the double-layered PAH doughnuts, in particular the larger ones (**52**, **62**), tend to display abnormally large polarizabilities, an observation which is clearly very reminiscent of those made for the $^1$H NMR chemical shifts of these systems. The same observation also holds for compound **64**. With regards to the tremendously spectacular enhancement of the in-plane and isotropic polarizabilities with system size in the **3F**–**42**–**52**–**62** series, the compounds in the latter study appear to be particularly promising for applications in optoelectronics and in the design of organic materials with extremely high electrical conductivities. For instance, the polarizabilities per benzenoid unit in the **52** species clearly exceed those of the graphite sheet **5F**. At this stage, it is thus worth making a comparison with the polarizabilities of molecules like naphthacene (tetracene), perylene, and pentacene, these three PAH compounds being used nowadays for preparing semiconducting organic thin films suited to the making of electronic devices.[103] At the B3LYP/6-31G (HF/6-31G) level of theory the values of the isotropic polarizability per benzenoid ring in these three molecules are only 63.7 (65.7), 66.1 (60.0), and 75.9 (71.4) bohr$^3$ per benzenoid ring, respectively.

Uncorrelated theoretical models such as the HF/6-31G level are not able to handle properly near-energy degeneracies in low band gap (metallic) systems. More specifically, HF calculations on low band gap systems often lead to artificially too strong geometrical distortions from the most symmetric point groups in order to prevent near-energy degeneracies through an opening or increase of the HOMO–LUMO gap. A classic example is that of the Peierls distortions in one-dimensional low band gap systems,[104–106] in straightforward analogy with the more familiar Jahn–Teller distortions observed for the radical cations of molecules with non-abelian symmetry point groups. In view of their more pronounced metallic nature, it is therefore not a surprise at all that, at such a level, all studied even-layered hollow PAH compounds display one imaginary vibrational frequency in their $D_{6h}$ symmetry point group. Thus, although these are artefacts resulting from the neglect of electron correlation, these imaginary frequencies indicating symmetry-breakings relate to a smaller HF HOMO–LUMO gap. They reflect therefore the more pronounced metallic nature of the **42**, **52**, **62**, and **64** species, a finding which corroborates the observations made previously with polarizabilities and NICS indices. Note that at the B3LYP/6-31G level compound **64** still has one imaginary frequency under the constraint of the $D_{6h}$ symmetry point group.

## Conclusion

We have systematically investigated a series of polycyclic aromatic hydrocarbons (PAHs) with hollow sites and found

  

that in even-layered PAH doughnuts the internal cavities are strongly aromatic in the magnetic sense, that is, are subject to significant screening of an external magnetic field by the induction of particularly strong ring currents, in particular in the layer directly adjacent to the central hole of the double-layered compounds, whereas odd-layered systems are magnetically only moderately aromatic.

Our work nonetheless confirms the statistically multidimensional nature of aromaticity and points out an inherent dichotomy between the magnetic indices of aromaticity, on the one hand, and those based on structural and energetic criteria on the other hand. Indeed, rather than strictly reflecting aromaticity from a geometrical or stability point of view, the abnormally large NMR chemical shifts we have found for even-layered systems should rather be regarded in this particular case as a consequence of the propensity of these systems to undergo electronic excitations and thus as markers of electronic conductivity in the metallic sense. In line with this revision, even-layered doughnuts, in particular the largest ones, were found to exhibit abnormally large polarizabilities. Also in line with a more pronounced metallic nature and the fact therefore that the electron density in such systems is naturally more prone to undergo symmetry-breaking, the geometrical structure of these species systematically deviate from the $D_{6h}$ point group at the HF level. Magnetically aromatic central holes in the PAHs investigated were shown by computations of aromatic stabilization energies to have no extra stabilization effect. On the contrary, either aromatic or nonaromatic holes should by themselves rather be regarded as local destabilizing defects in finite-sized graphite sheets.

## Acknowledgements

This research was partially supported by the Ministry of Education, Science, Sports, and Culture, a Grant-in-Aid for the COE project, Giant Molecules and Complex Systems, 2003 (B.H.). B.H. is also grateful to the JSPS for current financial support (P04118). M.S.D. acknowledges financial support from the FWO, the Flemish branch of the National Scientific Foundation in Belgium, and from the Bijzonder OnderzoeksFonds of Hasselt University.

[1] G. C. Smith, J. F. Sinski, *Appl. Spectrosc.* **1999**, *53*, 1459.
[2] P. M. V. B. Barone, R. S. Braga, A. Camilo, Jr., D. S. Galvão, *THEOCHEM* **2000**, *505*, 55.
[3] J. L. Weisman, T. J. Lee, F. Salama, M. Head-Gordon, *Astrophys. J.* **2003**, *587*, 256.
[4] X. Chillier, P. Boulet, H. Chermette, F. Salama, J. Weber, *J. Phys. Chem.* **2001**, *115*, 1769.
[5] F. Salama, *J. Mol. Struct.* **2001**, *563*, 19.
[6] P. Bréchignac, T. Pino, *Astron. Astrophys.* **1999**, *343*, L49.
[7] A. Shimizu, H. Tachikawa, *Electrochim. Acta* **2003**, *48*, 1727.
[8] C. D. Dimitrakopoulos, S. Purishotoman, J. Kymissis, A. Callegari, M. J. Shaw, *Science* **1999**, *283*, 822.
[9] F. Dötz, J. D. Brand, S. Ito, L. Gherghel, K. Müllen, *J. Am. Chem. Soc.* **2000**, *122*, 7707.
[10] C. D. Simpson, J. D. Brand, A. J. Berresheim, L. Przybilla, H. J. Räder, K. Müllen, *Chem. Eur. J.* **2002**, *8*, 1424.
[11] J. Wu, L. Gherghel, M. D. Watson, J. Li, Z. Wang, C. D. Simpson, U. Kolb, K. Müllen, *Macromolecules* **2003**, *36*, 7082.
[12] S. E. Stein, R. L. Brown, *J. Am. Chem. Soc.* **1987**, *109*, 3721.
[13] P. Du, F. Salama, G. H. Loew, *Chem. Phys.* **1993**, *173*, 421.
[14] K. Hiruta, S. Tokita, K. Nishimoto, *J. Chem. Soc., Perkin Trans. 2* **1985**, 1443.
[15] B. Hajgató, K. Ohno, *Chem. Phys. Lett.* **2004**, *385*, 512.
[16] C. Niederalt, S. Grimme, S. D. Peyerimhoff, *Chem. Phys. Lett.* **1995**, *245*, 455.
[17] J. V. Goodpaster, J. F. Harrison, V. L. McGuffin, *J. Phys. Chem.* **1988**, *92*, 3372.
[18] Y. Bito, N. Shida, T. Toru, *Chem. Phys. Lett.* **2000**, *328*, 310.
[19] M. S. Deleuze, *J. Chem. Phys.* **2002**, *116*, 7012.
[20] M. S. Deleuze, *J. Phys. Chem. A* **2004**, *108*, 9244.
[21] S. Hirata, T. J. Lee, M. Head-Gordon, *J. Chem. Phys.* **1999**, *111*, 8904.
[22] T. M. Halasinski, J. L. Weisman, R. Ruiterkamp, T. J. Lee, F. Salama, M. Head-Gordon, *J. Phys. Chem. A* **2003**, *107*, 3660.
[23] For some organic chemistry textbooks, see: K. P. C. Vollhart, N. E. Schore, *Organic Chemistry*, 2nd ed., W. H. Freeman and Company, New York, **1994**.
[24] M. Bühl, A. Hirsch, *Chem. Rev.* **2001**, *101*, 1153.
[25] R. V. Williams, *Chem. Rev.* **2001**, *101*, 1185.
[26] R. H. Mitchell, *Chem. Rev.* **2001**, *101*, 1301.
[27] J. A. N. F. Gomes, R. B. Mallion. *Chem. Rev.* **2001**, *101*, 1349.
[28] T. M. Krygowski, M. K. Cyrañski, *Chem. Rev.* **2001**, *101*, 1385.
[29] F. De Proft, P. Geerlings, *Chem. Rev.* **2001**, *101*, 1451.
[30] S. W. Slayden, J. F. Liebman, *Chem. Rev.* **2001**, *101*, 1541.
[31] L. J. Schaad, B. A. Hess, Jr., *Chem. Rev.* **2001**, *101*, 1465.
[32] S. Shaik, A. Shurki, D. Danovich, P. C. Hiberty, *Chem. Rev.* **2001**, *101*, 1501.
[33] E. Clar, *Polycyclic Hydrocarbons, Vols. I and II* Academic Press, London, **1963**.
[34] E. Clar, *The Aromatic Sextet*, Wiley, London **1972**.
[35] a) A. F. Pozharskii, A. T. Soldatenkov, A. R. Katritzky, *Heterocycles in Life and Society*, Wiley, New York, **1997**; b) A. R. Katritzky, K. Jug, D. C. Oniciu, *Chem. Rev.* **2001**, *101*, 1421.
[36] P. George, M. Trachtman, C. W. Bock, A. M. Brett, *J. Chem. Soc., Perkin Trans. 2* **1976**, 1223.
[37] R. C. Haddon, V. R. Haddon, L. J. Jackman, Nuclear Magnetic Resonance of Annulenes. *Topics in Current Chemistry, Vol. 16*, Springer, Berlin, **1971**, p. 2.
[38] J. A. Elvidge, L. M. Jackman, *J. Chem. Soc.* **1961**, 859.
[39] J. A. Elvidge, *J. Chem. Soc. Chem. Commun.* **1965**, 160.
[40] C. A. Coulson, J. A. N. F. Gomes, R. B. Mallion, *Mol. Phys.* **1975**, *30*, 713.
[41] C. A. Coulson, R. B. Mallion, *J. Am. Chem. Soc.* **1976**, *98*, 592.
[42] R. B. Mallion, *Pure Appl. Chem.* **1980**, *52*, 1541.
[43] J. A. N. F. Gomes, R. B. Mallion, *J. Org. Chem.* **1981**, *46*, 719.
[44] R. B. Mallion, *Nature* **1987**, *325*, 760.
[45] C. W. Haigh, R. B. Mallion, *Progress in Nuclear Magnetic Resonance Spectroscopy, Vol. 13*, Pergamon Press, Oxford, **1979/1980**, p. 303.
[46] J. A. N. F. Gomes, R. B. Mallion, *Concepts in Chemistry*, Research Studies Press Limited, Taunton (UK) and Wiley, New York, **1997**, Chapter 7. p. 205.
[47] P. Lazaretti, *Progress in Nuclear Magnetic Resonance Spectroscopy, Vol. 36*, Elsevier, Amsterdam, **2000**, p. 1.
[48] C. F. Wilcox, J. P. Uetrecht, G. D. Grantham, K. G. Grohmann, *J. Am. Chem. Soc.* **1975**, *97*, 1914.
[49] C. F. Wilcox, E. N. Farley, *J. Am. Chem. Soc.* **1984**, *106*, 7195.
[50] C. F. Wilcox, E. N. Farley, *J. Org. Chem.* **1985**, *50*, 351.
[51] a) C. W. Bird, *Tetrahedron* **1985**, *41*, 1409; b) C. W. Bird, *Tetrahedron* **1986**, *42*, 89; c) C. W. Bird, *Tetrahedron* **1987**, *43*, 4725.
[52] a) P. von R. Schleyer, P. K. Freeman, H. Jiao, B. Goldfuss, *Angew. Chem.* **1995**, *107*, 332; *Angew. Chem. Int. Ed. Engl.* **1995**, *34*, 337.
[53] L. Nyulászi, P. von R. Schleyer, *J. Am. Chem. Soc.* **1999**, *121*, 6872.

  

[54] For example, see: M. K. Cyrañski, T. M. Krygowski, A. R. Katritzky, P. von R. Schleyer, *J. Org. Chem.* **2002**, *67*, 1333, and references therein.
[55] H. Hosoya, K. Hosoi, I. Gutman, *Theor. Chim. Acta* **1975**, *38*, 37.
[56] R. B. Mallion, *Proc. R. Soc. London, Ser. A*, **1975**, *341*, 429.
[57] I. Gutman, *Bull. Soc. Chim. Beograd* **1982**, *47*, 453.
[58] I. Gutman, O. E. Polansky, *Mathematical Concepts in Organic Chemistry*, Springer, Heidelberg, **1986**.
[59] S. J. Cyvin, I. Gutman, *Kekulé Structures in Benzenoid Hydrocarbons: Lecture Notes in Chemistry, 46*, Springer, Heidelberg, **1988**.
[60] I. Gutman, S. J. Cyvin, *Introduction to the Theory of Benzenoid Hydrocarbons*, Springer, Heidelberg, **1989**, Chapter 7, p. 93.
[61] C. W. Haigh, R. B. Mallion, *Croat. Chem. Acta* **1989**, *61*, 1.
[62] M. Randić, *Chem. Rev.* **2003**, *103*, 3449.
[63] "Delocalization - Pi and Sigma", Complete 10th issue, *Chem. Rev.* **2005**, *105*, 3343–3947.
[64] F. Jensen, *Introduction to Computational Chemistry*, Wiley, Chichester, **1999**, Chapter 10.
[65] A. D. Buckingham, *Adv. Chem. Phys.* **1967**, *12*, 106.
[66] P. W. Fowler, *Annu. Rep. Prog. Chem., Sect. C* **1987**, *83*, 3.
[67] See, for example: J.-M. André, J. Delhalle, J.-L. Brédas, *Quantum Chemistry Aided Design of Organic Polymers*, World Scientific, Singapore, **1991**.
[68] Gaussian 03 (Revision C.02), M. J. Frisch, G. W. Trucks, H. B. Schlegel, G. E. Scuseria, M. A. Robb, J. R. Cheeseman, J. A. Montgomery, Jr., T. Vreven, K. N. Kudin, J. C. Burant, J. M. Millam, S. S. Iyengar, J. Tomasi, V. Barone, B. Mennucci, M. Cossi, G. Scalmani, N. Rega, G. A. Petersson, H. Nakatsuji, M. Hada, M. Ehara, K. Toyota, R. Fukuda, J. Hasegawa, M. Ishida, T. Nakajima, Y. Honda, O. Kitao, H. Nakai, M. Klene, X. Li, J. E. Knox, H. P. Hratchian, J. B. Cross, V. Bakken, C. Adamo, J. Jaramillo, R. Gomperts, R. E. Stratmann, O. Yazyev, A. J. Austin, R. Cammi, C. Pomelli, J. W. Ochterski, P. Y. Ayala, K. Morokuma, G. A. Voth, P. Salvador, J. J. Dannenberg, V. G. Zakrzewski, S. Dapprich, A. D. Daniels, M. C. Strain, O. Farkas, D. K. Malick, A. D. Rabuck, K. Raghavachari, J. B. Foresman, J. V. Ortiz, Q. Cui, A. G. Baboul, S. Clifford, J. Cioslowski, B. B. Stefanov, G. Liu, A. Liashenko, P. Piskorz, I. Komaromi, R. L. Martin, D. J. Fox, T. Keith, M. A. Al-Laham, C. Y. Peng, A. Nanayakkara, M. Challacombe, P. M. W. Gill, B. Johnson, W. Chen, M. W. Wong, C. Gonzalez, J. A. Pople, Gaussian, Inc., Wallingford CT, **2004**.
[69] J. Gerratt, I. M. Mills, *J. Chem. Phys.* **1968**, *49*, 1719.
[70] J. M. L. Martin, J. El-Yazal, J.-P. François, *Mol. Phys.* **1995**, *86*, 1437.
[71] M. S. Deleuze, M. G. Giuffreda, J.-P. François, *J. Phys. Chem. A* **2002**, *106*, 5626.
[72] P. von R. Schleyer, C. Maeker, A. Dransfeld, H. Jiao, N. J. R. van Eikema Hommes, *J. Am. Chem. Soc.* **1996**, *118*, 6317.
[73] P. von R. Schleyer, H. Jiao, N. J. R. van Eikema Hommes, V. G. Malkin, O. Malkina, *J. Am. Chem. Soc.* **1997**, *119*, 12669.
[74] See also Paragraph VI in ref. 27 (p. 1366).
[75] R. Ditchfield, *Mol. Phys.* **1974**, *27*, 789.
[76] M. J. Lacey, *Aust. J. Chem.* **1970**, *23*, 1421.
[77] S. P. Kwasniewski, J.-P. François, M. S. Deleuze, *Int. J. Quantum Chem.* **2000**, *80*, 672.
[78] M. W. Casida, C. Jamorski, K. C. Casida, D. R. Salahub, *J. Chem. Phys.* **1988**, *88-89*, 4439.
[79] D. J. Tozer, N. C. Handy, *J. Chem. Phys.* **1998**, *109*, 10180.
[80] S. Grimme, M. Parac, *ChemPhysChem* **2003**, *4*, 292.
[81] P. Otto, A. Martinez, A. Czaja, J. Ladik, *J. Chem. Phys.* **2002**, *117*, 1908.
[82] S. Suhai, *Chem. Phys. Lett.* **1983**, *96*, 619.
[83] S. Suhai, *Phys. Rev. B* **1983**, *27*, 3506.
[84] M. S. Miao, P. E. Van Camp, V. E. van Doren, J. J. Ladik, J. W. Mintimre, *J. Chem. Phys.* **1998**, *109*, 9623.
[85] O. Kwon, M. L. McKee, *J. Phys. Chem. B* **2000**, *104*, 1686.
[86] P. R. Rablen, S. A. Pearlman, J. Finkbiner, *J. Phys. Chem. A* **1999**, *103*, 7357.
[87] B. Wang, U. Fleischer, J. F. Hinton, P. Pulay, *J. Comput. Chem.* **2001**, *22*, 1887.
[88] a) F. Diederich, H. A. Staab, *Angew. Chem.* **1978**, *90*, 383; *Angew. Chem. Int. Ed. Engl.* **1978**, *17*, 372.
[89] J.-M. Gilles, J. F. M. Oth, F. Sondheimer, E. P. Woo, *J. Chem. Soc. B* **1971**, 2177.
[90] a) E. Steiner, P. W. Fowler, L. W. Jenneskens, *Angew. Chem.* **2001**, *113*, 375; *Angew. Chem. Int. Ed.* **2001**, *40*, 362.
[91] E. Steiner, P. W. Fowler, L. W. Jenneskens, A. Acocella, *Chem. Commun.* **2001**, 659.
[92] J. Aihara, *Chem. Phys. Lett.* **2002**, *365*, 34.
[93] J. Aihara, *Chem. Phys. Lett.* **2004**, *393*, 7.
[94] V. Elser, R. C. Haddon, *Nature* **1987**, *325*, 792.
[95] NBO (Version 3.1), E. D. Glendening, A. E. Reed, J. E. Carpenter, F. Weinhold, Madison, **1988**.
[96] We omitted **62b**, **63b**, and **64b** from this table because the optimization at the CNDO level of theory leads to the planar $D_{6h}$ symmetry form. The CIS-ZINDO-S//B3LYP/6-31G $S_0$–$S_1$ transitions are the same for the planar and the corresponding bowl-shaped forms and are 0.34, 1.80, and 0.80 eV for **62**/**62b**, **63**/**63b**, and **64**/**64b**, respectively.
[97] B. R. M. de Castro, J. A. N. F. Gomes, R. B. Mallion, *J. Mol. Struct.* **1992**, *265–275*, 123.
[98] B. R. M. de Castro, J. A. N. F. Gomes, R. B. Mallion, *J. Mol. Struct.* **1992**, *265–275*, 133.
[99] B. R. M. de Castro, J. A. N. F. Gomes, R. B. Mallion, *Croat. Chem. Acta* **1993**, *65*, 49.
[100] X. Yang, B. Hajgató, M. Yamada, K. Ohno, *Chem. Lett.* **2005**, *34*, 506.
[101] W. Gordy, *J. Chem. Phys.* **1947**, *15*, 305.
[102] M. Randiæ, *Chem. Phys. Lett.* **1976**, *38*, 68.
[103] S. Verlaak, S. Steudel, P. Heremans, D. Janssen, M. S. Deleuze, *Phys. Rev. B* **2003**, *68*, 195409.
[104] R. E. Peierls, *Quantum Theory of Solids*, Clarendon Press, Oxford, **1955**.
[105] V. V. Walatka, M. M. Labes, J. H. Perlstein, *Phys. Rev. Lett.* **1973**, *31*, 1139.
[106] L. Greene, G. B. Street, L. J. Suter, *Phys. Rev. Lett.* **1977**, *38*, 1305.

Received: October 24, 2005
Revised: February 10, 2006
Published online: May 23, 2006

  